Monthly Notices
of the
ROYAL ASTRONOMICAL SOCIETY

Mon. Not. R. Astron. Soc. **405,** 695–700 (2010) doi:10.1111/j.1365-2966.2010.16492.x

The long rapid decay phase of the extended emission from the short GRB 080503

F. Genet,[1,2]★ N. R. Butler[3] and J. Granot[1]

[1]*Centre for Astrophysics Research, University of Hertfordshire, Hatfield AL10 9AB*
[2]*Racah institute of Physics, Hebrew University, 91904 Jerusalem, Israel*
[3]*Astronomy Department, University of California, Berkeley, CA 94720-7450, USA*

Accepted 2010 February 7. Received 2010 February 4; in original form 2009 November 7

ABSTRACT

GRB 080503 was classified as a short gamma-ray burst (GRB) with extended emission. The origin of such extended emission (found in about a quarter of *Swift* short GRBs) is still unclear and may provide some clues to the identity of the elusive progenitors of short GRBs. The extended emission from GRB 080503 is followed by a rapid decay phase (RDP) that is detected over an unusually large dynamical range (one decade in time and ∼3.5 decades in flux), making it ideal for studying the nature of the extended emission from short GRBs. We model the broad envelope of extended emission and the subsequent RDP using a physical model for the prompt GRB emission and its high latitude emission tail, in which the prompt emission (and its tail) is the sum of its individual pulses (and their tails). For GRB 080503, a single pulse fit is found to be unacceptable, even when ignoring short time-scale variability. The RDP displays very strong spectral evolution and shows some evidence for the presence of two spectral components with different temporal behaviour, likely arising from distinct physical regions. A two pulse fit (a first pulse accounting for the gamma-ray extended emission and decay phase, and the second pulse accounting mostly for the X-ray decay phase) provides a much better (though not perfect) fit to the data. The shallow gamma-ray and steep hard X-ray decays are hard to account for simultaneously, and require the second pulse to deviate from the simplest version of the model we use. Therefore, while high latitude emission is a viable explanation for the RDP in GRB 080503, it does not pass our tests with flying colours, and it is quite plausible that another mechanism is at work here. Finally, we note that the properties of the RDP following the extended emission of short GRBs (keeping in mind the very small number of well-studied cases so far) appear to have different properties than that following the prompt emission of long GRBs. However, a larger sample of short GRBs with extended emission is required before any strong conclusion can be drawn.

Key words: radiation mechanisms: non-thermal – gamma-rays: bursts.

1 INTRODUCTION

GRB 080503 was detected by the *Swift* Burst Alert Telescope (BAT) on 2008 may 3 (Perley et al. 2009). Its prompt gamma-ray emission presents a short (∼0.32 s) intense initial spike followed by an extended emission lasting several minutes, for a total duration of $T_{90} \approx 232$ s. The first short spike duration in the 15–150 keV band is 0.32 ± 0.07 s and its peak flux is $(1.2 \pm 0.2) \times 10^{-7}$ erg cm^{-2} s^{-1}. The count rate hardness ratio between the 50–100 keV and the 25–50 keV of the initial spike is 1.2 ± 0.3, consistent with other short *Swift* bursts, but also with some long bursts. The fluence of the extended emission (measured between 5 and 140 s) in the 15–150 keV band is $(1.86 \pm 0.14) \times 10^{-6}$ erg cm^{-2}, about 30 times that of the initial spike, higher than for any other short *Swift* bursts, but within the range of such ratio measured for BATSE short bursts. Perley et al. (2009) found a spectral lag between the 50–100 keV and the 25–50 keV bands consistent with zero. All these led them to associate GRB 080503 with the 'short' (Kouveliotou et al. 1993) class.

The *Swift* X-Ray Telescope (XRT) started observing GRB 080503 about 82 s after the burst, detecting a bright early afterglow that rapidly decayed ($\alpha = 2$–4 with $F_\nu \propto t^{-\alpha}$) to below the detection threshold during the first orbit, which makes a record overall decline of ∼6.5 decades, with a steep decay clearly observed for ∼3.5 decades (see fig. 6 of Perley et al. 2009). *Chandra* detections at ∼3 d after the gamma-ray burst (GRB) indicate the presence

★E-mail: f.genet@herts.ac.uk

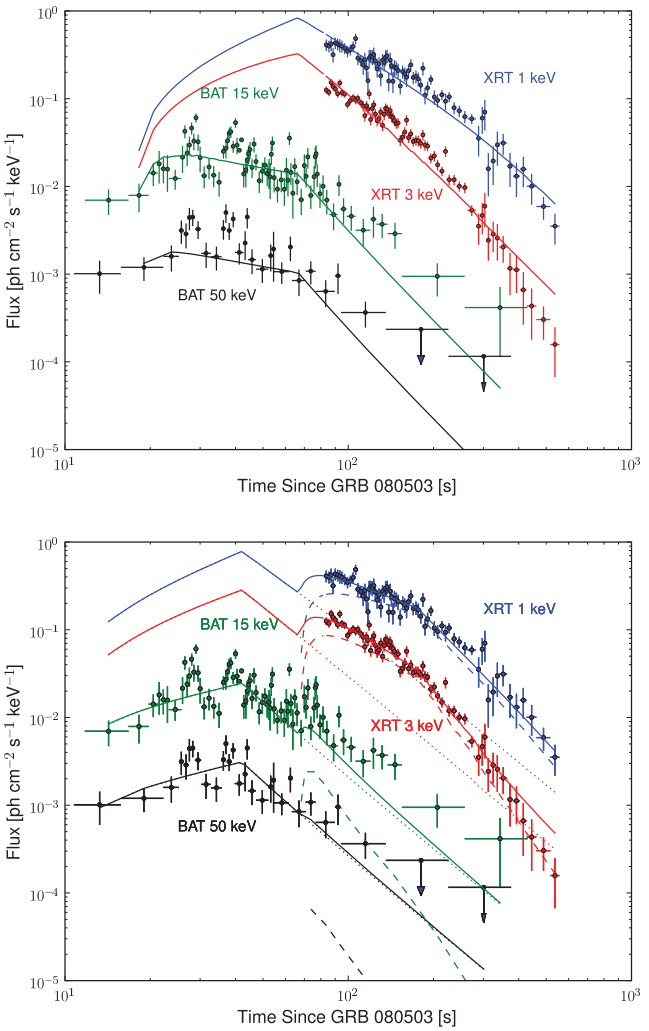

Figure 1. One- (top) and two- (bottom) component model fits to the early GRB 080503 data from the *Swift* BAT and XRT. The scaling of the counts data to flux units (y-axis) is approximate; however, the model fitting appropriately convolves the time-dependent input spectrum through the instrumental response matrices. In the bottom panel, dotted and dashed lines show the two components separately, while the solid curves show the sum of the two components. The best-fitting parameters are shown in Tables 1 and 2.

of a separate X-ray afterglow component $\sim 10^6$ times fainter than the peak emission from the X-ray tail of the prompt extended emission. The gamma-ray light curve of the extended emission (which can be found with the X-ray light curve of the extended emission in Fig. 1) presents two relatively well-defined spikes at $\sim$28 and $\sim$36 s, followed by some less-defined variability with several narrow spikes (see also fig. 1 of Perley et al. 2009). The X-ray rapid decay phase (RDP) light curves present a first break at $\sim$180 s seen in both soft and hard bands; later on, the hard X-ray band clearly shows a steepening (to a temporal slope of about -4.2) that is only marginally seen in the soft X-rays. The simultaneous gamma-ray decay is much shallower, with a temporal slope only about -2.

The RDP of GRB 080503 is a smooth temporal and spectral continuation of the extended emission in the gamma-rays (Perley et al. 2009). This suggests that it is the tail of the prompt emission (O'Brien et al. 2006; Butler & Kocevski 2007). The most popular model to explain the RDP following the prompt emission of long GRBs is high latitude emission (HLE; Kumar & Panaitescu 2000). In this model, after the prompt emission stops, photons from increasingly larger angles relative to the line of sight still reach the observer, due to the curvature of the (assumed to be quasi-spherical) emitting surface. The blueshift of such photons decreases with the angle from the line of sight, and therefore with their arrival time. This results in a simple relation between the temporal and spectral indices of the flux, $\alpha = 2 + \beta$, where $F_\nu \propto t^{-\alpha}\nu^{-\beta}$, that holds at late times (when $t - t_0 \gg \Delta t$, where t_0 is the onset time of the pulse and Δt its width) for each pulse of the prompt emission.

The RDP following the extended emission of the short GRB 080503, however, shows strong spectral evolution that is different than that typically seen in the RDP following the prompt emission of long GRBs. Whereas in the latter case, the RDP usually shows a monotonic softening of the spectrum with time (see Zhang, Liang & Zhang 2007, and references therein), the RDP in GRB 080503 shows a similar softening in the XRT energy range together with a hardening in the spectral slope between the XRT and the BAT energy ranges. This behaviour suggests the presence of two distinct spectral components.

Such extended emission is observed in about a quarter of short *Swift* bursts (Norris & Gehrels 2009; Norris, Gehrels & Scargle 2009). It usually lasts tens of seconds, and has been shown to be always softer than the initial short spike, however showing negligible lags as the initial spike (Norris & Bonnel 2006). The same authors also found that the extended emission is softer than the initial spike, making it closer to long bursts, which are softer than short bursts. However, the initial spike of short bursts with and without extended emission show similar properties (Norris & Gehrels 2009). Many authors recently turned to environmental constraints to explain differences between short GRBs with and without EE, but with results at best uncertain, sometime contradictory (Troja et al. 2008; Nysewander, Fruchter & Pe'er 2009; Sakamoto & Gehrels 2009; Fong, Berger & Fox 2010; Rhoads 2010). There is as of now no strong explanation for the mechanism behind extended emission. It is therefore very important to test whether HLE can indeed explain the RDP of GRB 080503, as this would allow some comparison with results for the RDP following the prompt emission without extended emission (Willingale et al. 2010). This will stress similarities and differences between the extended emission and the prompt emission itself, ultimately leading to a better understanding of the origin of extended emission.

Genet & Granot (2009, hereafter GG09) have developed a simple yet physical and self-consistent model for the prompt and HLE. The very large dynamical range over which the RDP of GRB 080503 is observed allows us to test its behaviour at late times, which is rarely possible in other *Swift* bursts. In order to test whether the extended emission is coming from a mechanism similar to the prompt emission itself, we apply the GG09 model to GRB 080503 data by folding it through the response matrices generated from the four energy bands of data (0.3–1.3 and 1.3–10.0 keV for the XRT; 15–50 and 50–150 keV for the BAT). Section 2 summarizes the theoretical model used to fit the burst light curves. Section 3 describes how the data are reduced and fitted, and the results of our fits. In Section 4, we discuss the implications of these results.

2 THE THEORETICAL MODEL

The prompt and extended emissions and their tail (the RDP) are taken to be the sum of its pulses and their tails, as described in GG09. Each pulse represents a single emission episode, assumed to come from an ultra-relativistic ($\gamma \gg 1$) thin spherical

expanding shell, turns on at radius R_0 and turns abruptly off at radius $R_f \equiv R_0 + \Delta R$, where ΔR is the width of the emission region. The emission is assumed to be uniform over the emitting shell and isotropic in its rest frame. The observed flux is calculated by integrating over the surface of equal arrival time of photons to the observer (following Granot 2005 and Granot, Cohen-Tanugi & do Couto e Silva 2008). The characteristic observed times of a pulse are the ejection time of the emitting shell (T_{ej}), the radial time at R_0 (T_0) and at R_f [$T_f \equiv T_0(1 + \Delta R/R_0)$]; T_f is also essentially the temporal width of the pulse. For $\Delta R/R_0 \lesssim$ a few, the peak of the pulse is observed at $T_{peak} = T_{ej} + T_f$. We consider that the peak luminosity of the shell evolves as $L'_{\nu'_p} \propto R^a$. In the case of emission by synchrotron mechanism from electrons accelerated in internal shocks and cooling fast, $a = 1$, but in the following it will be kept free as fixing its value does not simplify the calculations, and it allows to check for deviations from these assumptions. In this framework, we also have the peak frequency of the νF_ν spectrum evolving as $\nu'_p \propto R^{-1}$. The emission spectrum is assumed to be the phenomenological Band function (Band et al. 1993). The number of photons N per unit photon energy E, area A and observed normalized time $\tilde{T} \equiv (T - T_{ej})/T_0$ of a single emission episode is then [where we also define $\tilde{T}_f \equiv (T_f - T_{ej})/T_0$]:

$$\frac{\mathrm{d}N}{\mathrm{d}E\,\mathrm{d}A\,\mathrm{d}T}(E, \tilde{T} \geq 1) = \tilde{T}^{-1}\left[\min(\tilde{T}, \tilde{T}_f)^{a+2} - 1\right] B\left(\frac{E}{E_0}\tilde{T}\right),$$

where a is kept free to vary as fixing its value does not simplify calculations and

$$B(z) = B_{norm}\begin{cases} z^{-1-\beta_l}\mathrm{e}^{-z} & z \leq \Delta\beta \\ z^{-1-\beta_h}(\Delta\beta)^{\Delta\beta}\mathrm{e}^{-\Delta\beta} & z \geq \Delta\beta \end{cases}$$

is the Band function with a normalization constant B_{norm}, with high- and low-energy photon indices of $-1 - \beta_h$ and $-1 - \beta_l$, respectively, where $\Delta\beta = \beta_h - \beta_l$ and $z = (E/E_0)\tilde{T}$. One can remark that the observed spectrum is a Band function spectrum, as the emitted one, but with its peak energy sweeping through the observed bands: the peak of $E^2\,\mathrm{d}N/\mathrm{d}E$ is $E_{peak} = (1 - \beta_l)E_0/\tilde{T}$, where $E_0 \equiv E_{peak}(\tilde{T} = 1)/(1 - \beta_l)$, which decreases linearly with the normalized time $\tilde{T}$. At times $\tilde{T} \geq \tilde{T}_f$ is observed the HLE of the shell. In this part of the light curve of the pulse, the spectral slope $-\mathrm{d}\log(E^2\,\mathrm{d}N/\mathrm{d}t\,\mathrm{d}E\,\mathrm{d}A)/\mathrm{d}\log E$ will evolve from $1 - \beta_l - \tilde{T}\,E_{obs}/E_0$ (where E_{obs} is the observed photon energy) to $1 - \beta_h$, if $E_{obs} < E_0$. This creates a break in the light curve, which becomes very smooth if the observations are done in an energy band of finite width.

3 DATA REDUCTION AND FITTING

We download the raw, unfiltered *Swift* BAT and XRT data for GRB 080503 from the *Swift* Archive.[1] Our reduction of these data to science quality light curves and spectra are detailed in Perley et al. (2009). Here, we subdivide the X-ray and γ-ray light curves into much finer time bins to study the spectral evolution. We begin with the BAT 15–350 keV and XRT 0.3–10.0 keV light curves, with each bin containing sufficient counts to reach a signal-to-noise ratio (S/N) of 3 or greater. We then generate response matrices for each time bin, using the tools summarized in Perley et al. (2009). Our reduction accounts for the spacecraft slew for BAT as well as photon pileup for the XRT, among other effects.

Table 1. One-component model: best-fitting parameters.

One-component model	
Parameter	Value
β_l	-0.67 ± 0.18
β_h	1.13 ± 0.08
t_f (s)	55.35 ± 2.99
t_{peak} (s)	66.56 ± 3.30
$\mathrm{d}R/R$	8.33 ± 1.43
$\log E_0(t_{peak})$	0.59 ± 0.09
N_H (cm^{-2})	$(8.7 \pm 2.2) \times 10^{20}$
a	0.67 ± 0.17
$\log \sigma_0$ (BAT and XRT)	-1.27 ± 0.08

Next, we further subdivide the BAT and XRT data each into soft and hard energy channels: 15–50 and 50–150 keV for BAT; 0.3–1.3 and 1.3–10.0 keV for the XRT. We rebin the data (and group the response matrices accordingly) so that each hard and soft channel still has S/N $\geq$ 3. The soft- and hard-channel light curves are shown in Fig. 1. To fit the temporal/spectral model of GG09 to the two-energy-channel BAT and XRT data as a function of time, we fold the model through the response matrices at each time bin and minimize the total χ^2. Fitting is accomplished using Markov Chain Monte Carlo through the python PYMC package.[2]

At the beginning of the RDP, the flux is expected to be dominated by the last pulse. However, at later times other pulses are expected to become dominant, and the contribution of each pulse to the flux at late times ($t - t_0 \gg \Delta t$) scales as $\sim F_{peak} T_f^{2+\beta}$ when β is constant among the pulses: higher (with a larger F_{peak}) or wider (with a larger T_f) pulses will dominate. The width of the pulse having a larger power ($2 + \beta \sim 4$–5 for $\beta \sim 2$–3) in the relative contribution to the flux, it will be the most important parameter to find the dominant pulse. This is not true if the high-energy spectral slope is varying among pulses, but we assume that such variations are small enough so that the contribution at late times of narrow pulses are still small compared to larger ones. Given the shape of the BAT light curve of GRB 080503, it thus seems most natural to explain it by one or two broad pulse(s) superimposed by narrower ones that would account for the smaller time-scale variability observed (such as the spikes at 28 and 36 s), but whose contribution to the RDP would be negligible: the ratio of their width being of the order of $10/60 \approx 0.16$, the ratio of their contribution to the tail of the prompt emission would be about $0.16^4 \approx 7 \times 10^{-4}$ or less. The results presented here will describe only the broad pulse(s) fitting and results, as in it lay the most important physics.

3.1 Single pulse model

We begin by fitting a single pulse BAT emission model to study the expected late-time emission in the XRT bands. Initial temporal parameters (rise time t_f and peak time t_{peak}) are chosen to crudely reproduce an envelope of emission containing the BAT light curve. We then allow these and the other model parameters to vary (Table 1).

We find that a single pulse model tends to yield a mediocre fit to the data. The fit requires a systematic error term (in addition to the measured error) of 30 per cent in order to yield $\chi^2 = \nu$. This error is not driven by the BAT time variability alone (although it

[1] ftp://legacy.gsfc.nasa.gov/swift/data

[2] http://code.google.com/p/pymc

Table 2. Two-component model: best-fitting parameters.

Parameter	Two-component model 1st pulse	2nd pulse
$\beta_{\rm l}$	0 (fixed)	
$\log norm.$	-4.69 ± 1.19	-0.89 ± 0.47
$\beta_{\rm h}$	0.63 ± 0.08	2.13 ± 0.33
$t_{\rm f}$ (s)	37.23 ± 2.45	125.67 ± 10.37
$t_{\rm peak}$ (s)	42.12 ± 2.24	176.35 ± 9.11
a	1.311 ± 0.26	-0.38 ± 0.19
$\log E_0$	1.0 ± 0.3	0.3 ± 0.1
dR/R	6.67 ± 0.39	
$N_{\rm H}$ (cm^{-2})	$(2.0 \pm 0.4) \times 10^{21}$	
$\log \sigma_0$	-1.63 ± 0.10	

contributes). There is clear difficulty in fitting the smooth light-curve break in the X-ray bands and also potentially in fitting the high flux in the BAT after $t \approx 150$s. However, we note that the error bars on the late-time BAT flux are large. The limits plotted in Fig. 1 (top) for the BAT hard channel are at the 2σ level.

3.2 Double pulse model

Because the single pulse model has difficulty reconstructing the slow BAT decline as well as the rapid X-ray break, we attempt fitting a model with two pulses. As displayed in Fig. 1 (bottom), the data are considerably better fit with two pulses, the parameters for which are given in Table 2. In the fitting, we tie several of the parameters from pulse B to those from pulse A. We also fix the low-energy Band model index $\beta_{\rm l} = 0$, which is typical for GRBs. A large value for that index from the single pulse model may further suggest the inappropriateness of that model.

The data are fitted by a soft early pulse (peaking at $t = 42$ s with $E_0 = 1.0$ keV) and a softer later pulse (peaking at $t = 175$ s with $E_0 = 0.3$ keV). The BAT emission is dominated by the early pulse, whereas the late pulse provides the temporal break observed in the XRT bands around 185 s, which in this case is the beginning of the high latitude decay of the second pulse.

We have attempted fits of three or more pulses to the data as well. These do not appear to significantly improve the fit, which even for the two pulse model requires a 20 per cent systematic uncertainty. Apart from the possible slow BAT decay at $t > 150$ s, this extra uncertainty appears to be needed to account for light curve variability, which is not treated in the model.

4 DISCUSSION

The main problem in fitting the data with a single pulse is the very steep decay of the hard X-ray band combined with the relatively shallow decay of the BAT bands. In order to find a reason for such a behaviour, we extracted spectra at different time intervals (80–100, 100–150, 150–290 and 290–345 s) along the RDP light curve (when data in the four BAT and XRT bands are available) to probe the spectral evolution (see Fig. 2, where from earliest to latest spectra the colours are black, dark blue, red and cyan). Although the data are marginally consistent with a Band function with constant slopes and decreasing $E_{\rm peak}$, there is evidence for a departure from a Band spectrum to a spectrum with a concave shape beginning at $t \gtrsim 150$ s. Such spectral evolution would strongly suggest that at times $\gtrsim$150 s, a second component contributes to the flux; this would naturally

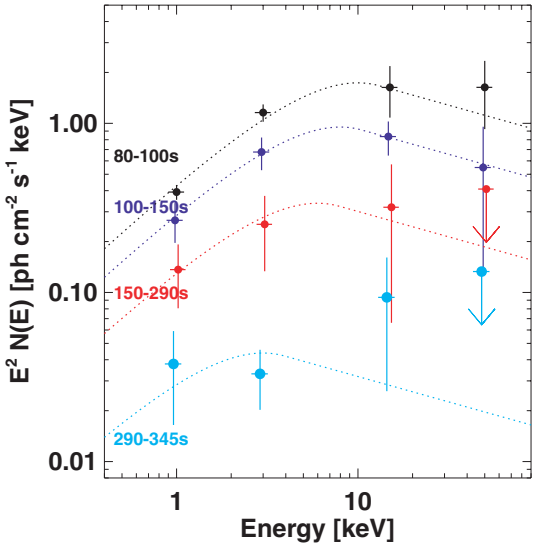

Figure 2. Spectra of GRB 080503 at different time interval during the RDP when both gamma-ray and X-ray are observed: 80–100 s (black), 100–150 s (dark blue), 150–290 s (red) and 290–345 s (cyan). The dotted curves show for comparison a Band function spectrum with $\beta_{\rm l} = 0$, $\beta_{\rm h} = 1.3$, and $F_\nu(E_{\rm peak}) \propto E_{\rm peak}^2$, which is roughly expected from HLE.

explain the distinct X-ray and gamma-ray behaviours of the RDP, accounting for the rapid X-ray decline and slow gamma-ray decay.

The fit with two pulses gives much better results, as expected, since two physical components seem to contribute to the flux. In this two pulse modelling, the first part of the emission ($t \lesssim 65$ s) is accounted for by a first pulse, and the second part, including the whole RDP, by the second component. The X-ray break at ∼185 s is the start of the high latitude decay of the second pulse, and the smooth break along the rest of the RDP is due to the sweeping up of the peak energy of the spectrum across the observed energy bands (as explained in Section 2). Due to the reappearance at late time ($t \gtrsim 300$ s) of the first component above the second one, the steep decay in the hard X-ray band is still not very well accounted for. However, when looking at the four-points spectra, one can see that the high- and low-energy slopes seem to change (on top of the appearance of a second component): from the earliest to the latest spectrum, the low-energy slope seems to decrease with time (the low-energy slope of the νF_ν spectrum becomes shallower with time), and the high-energy slope also seems to steepen. This may explain why the introduction of a second component alone (with fixed Band function parameters) cannot reproduce both the steep hard X-ray and the slow gamma-ray decline, even with a very steep high-energy photon index ($\beta_{\rm h} \approx 2.13$); evolution of the Band function slopes seem required.

The slow gamma-ray decay could alternatively be due to a series of spikes that are reasonably narrow (with $\Delta t < t$), unresolved (due to the wide late time BAT time bins) and hard (dominating at soft gamma-rays but with a small X-ray flux), so that we see only their smooth envelope, while their tail would hardly contribute to the observed X-ray decay. We do not directly model this, however, since it would introduce far too many new free parameter, and thus not provide a very stringent test for such a model.

We had kept a as a free parameter since it did not complicate the modelling and could test for deviations from its simplest form. Indeed, none of the values obtained for the fits is perfectly consistent with 1. Considering only the two pulse fit (the one pulse fit not being good enough to have any physical significance), the values

Table 3. Dependence of the parameters a and d (with $L'_{\nu'_p} \propto R^a$ and $\nu'_p \propto R^d$) on u (with the strength of the shocks in the outflow being parametrized by the relative upstream to downstream four-velocity as $U_{ud} \propto R^u$), and values of u and d for the fitted value $a_2 = -0.38 \pm 0.19$ of the second pulse of the two pulses model.

	Equipartiton field	
	$u \ll 1$	$u \gg 1$
$a(u)$	$1 - 2u$	$1 - 2u$
$d(u)$	$5u - 1$	$3u - 1$
$u(a_2)$	0.69 ± 0.095	0.69 ± 0.095
$d[u(a_2)]$	2.45 ± 0.475	1.07 ± 0.285
	Advected field	
$a(u)$	$1 - u$	$1 - 2u$
$d(u)$	$4u - 1$	$3u - 1$
$u(a_2)$	1.38 ± 0.19	0.69 ± 0.095
$d[u(a_2)]$	4.52 ± 0.76	1.07 ± 0.285

of a for the first and second pulses (pulse number indicated by a subscript number) are $a_1 = 1.31 \pm 0.26$ and $a_2 = -0.38 \pm 0.19$. Since the value $a = 1$ was obtained under the assumptions of electrons cooling fast by synchrotron emission in a coasting outflow, this means that at least one of the above assumptions is not true in the case of GRB 080503. The most natural assumption to relax is that the strength of the shocks in the outflow is constant. Assuming that it varies with radius, namely parametrizing the relative upstream to downstream four-velocity as $U_{ud} \propto R^u$ (while the Lorentz factor of the emitting shocked region remains constant), then $a = a(u)$ and $d = d(u)$, where $L'_{\nu'_p} \propto R^a$ and $\nu'_p \propto R^d$. The dependence of a and d on u are summarized in Table 3, where we have considered two options for the magnetic field in the emitting region: (i) a field strongly amplified at the shock that holds a constant fraction ϵ_B of the internal energy (equipartition) and (ii) a pre-existing magnetic field advected from the central source (scaling as R^{-1} upstream) and merely compressed at the shock (advected field). The values of the parameters u and d corresponding to the value $a_2 = -0.38 \pm 0.19$ of the second pulse are given as well (since the value of a for the first pulse is close to its fiducial value $a = 1$). One can note that the value of a inferred from the fit implies a value of $d > 1$, meaning that ν'_p rises with radius at least linearly, which is very different from the basic model where $\nu'_p \propto R^{-1}$. We stress, however, that the parameters a and d affect mainly the rising parts of the pulses and hardly affect the decaying parts. Since we do not have strong constraints on the time variation of the peak frequency during the rising parts of the pulses, parameter values similar to the ones we infer may be able to reasonably fit the data.

5 CONCLUSION

We have explored the extended emission and very long RDP of GRB 080503 in the light of the realistic physically motivated model for the prompt and latitude emission from GG09. Neglecting narrow pulses that do not affect the HLE, we fitted the broad underlying envelope of the extended emission and its RDP, expecting a simple HLE behaviour, motivated by the results of Perley et al. (2009). The first attempt, using a single pulse, failed to account for both the slow gamma-ray and very rapid hard X-ray declines. A close look at the spectral evolution during the RDP (at times $\gtrsim$150 s) showed evidence of a strong spectral evolution; the emergence of a second spectral component dominating the high energies is spotted, as well as evolution of the spectral slopes of the (assumed) Band function spectrum. This led us to fit the data with two pulses, the first one accounting for the gamma-ray envelope and decay phase, the second one accounting for the X-ray decay phase. The fit thus obtained is far better, even if not perfect, since we are still not accounting for the smaller variability. Adding a third pulse does not improve the fit, which suggests two pulses are enough to account for the data (as suggested by the spectral evolution). However, the fit we obtained is still far from perfect (the hard X-ray decay is still too steep at the latest times), the model being unable to account for the evolution of spectral slopes, and the fitting results showing discrepancies with its simplest form. This points out that the simplest form of GG09 model for HLE is not detailed enough to account for the complex RDP of GRB 080503. The mechanism at work here may thus still be HLE, but since this model has some difficulties and requires many degrees of freedom in order to produce a reasonable fit, this may suggest that another mechanism might be at the origin of the RDP in GRB 080503.

A previous attempt at fitting GG09 model to a short pulse with extended emission was done on GRB 050724 by Willingale et al. (2010). They also could not obtain a good fit of the extended emission in both BAT and XRT band, the model not being able to account for a slow BAT decay and a steep XRT decay during the RDP – similarly to what is observed with GRB 080503. Such feature may thus be a characteristic of RDP from extended emission, but more bursts should be studied before any conclusion can be drawn. Willingale et al. (2010) argue that HLE is a valid explanation for the RDP of GRBs without extended emission. If there is indeed a difference in the RDP of bursts with and without extended emission, then the properties of extended emission would be different from the prompt emission, which might suggest that they have a different physical origin. GRB 080503 may thus be the first stone paving the way to a better understanding of extended emissions in GRBs by studying their RDP. However, one should keep in mind that on top of having been studied more carefully than other bursts, the RDP of GRB 080503 is uncommonly long, meaning that maybe the range on which rapid decay is usually observed is not large enough to show deviations from the high latitude decay. In this case, this should be taken as a caveat for drawing conclusions from model fitting to the RDP of GRBs.

ACKNOWLEDGMENTS

NRB is supported through the GLAST Fellowship Program (NASA Cooperative Agreement: NNG06DO90A). JG gratefully acknowledges a Royal Society Wolfson Research Merit Award.

REFERENCES

Band D. et al., 1993, ApJ, 413, 281
Butler N. R., Kocevski D., 2007, ApJ, 668, 400
Fong W., Berger E., Fox D. B., 2010, ApJ, 708, 9
Genet F., Granot J., 2009, MNRAS, 399, 1328 (GG09)
Granot J., 2005, ApJ, 631, 1022
Granot J., Cohen-Tanugi J., do Couto e Silva E., 2008, ApJ, 677, 92
Kouveliotou C., Meegan C. A., Fishman G. J., Bhat N. P., Briggs M. S., Koshut T. M., Paciesas W. S., Pendleton G. N., 1993, ApJ, 413, L101
Kumar P., Panaitescu A., 2000, ApJ, 541, L51
Norris J. T., Bonnell J. T., 2006, ApJ, 643, 266

Norris J. P., Gehrels N., 2008, in Galassi M., Palmer D., Fenimore E., eds, AIP Conf. Proc. Vol. 1000, Gamma-Ray Bursts 2007: Proceedings of the Santa Fe Conference. Am. Inst. Phys., New York, p. 280
Norris J. P., Gehrels N., Scargle J. D., 2009, ApJ, submitted
Nysewander M., Fruchter A. S., Pe'er A., 2009, ApJ, 701, 824
O'Brien P. T. et al., 2006, ApJ, 647, 1213
Perley D. A. et al., 2009, ApJ, 696, 1871
Rhoads J. E., 2010, ApJ, 709, 664
Sakamoto T., Gehrels N., 2009, in Meegan C., Gehrels N., Kouveliotou C., eds, AIP Conf. Proc. Vol. 1133, Gamma-Ray Bursts: Sixth Huntsville Symposium. Am. Inst. Phys., New York, p. 112
Troja E., King A. R., O'Brien P. T., Lyons N., Cusumono G., 2008, MNRAS, 385, L10
Willingale R., Genet F., Granot J., O'Brien P., 2010, MNRAS, doi: 10.1111/j.1365-2966.2009.16187.x
Zhang B. B, Liang E. W., Zhang B., 2007, ApJ, 666, 1002

This paper has been typeset from a TEX/LATEX file prepared by the author.